Atmospheric Blocking and Atlantic Multi-decadal Ocean Variability

Sirpa Häkkinen[1], Peter B. Rhines[2] and Denise L. Worthen[3]

[1] NASA Goddard Space Flight Center, Code 614.1, Greenbelt, MD 20771

[2] Univ. of Washington, Box 357940, Seattle, WA 98195

[3] WYLE ITS Systems/NASA Goddard Space Flight Center, Code 614.1, Greenbelt, MD 20771

Corresponding author e-mail: sirpa.hakkinen@nasa.gov

Brief summary:

Based on the 20th century atmospheric reanalysis, winters with more frequent blocking, in a band of blocked latitudes from Greenland to Western Europe, are found to persist over several decades and correspond to a warm North Atlantic Ocean, in-phase with Atlantic multi-decadal ocean variability.

Atmospheric blocking over the northern North Atlantic, which involves isolation of large regions of air from the westerly circulation for 5 days or more, influences fundamentally the ocean circulation and upper ocean properties by impacting wind patterns. Winters with clusters of more frequent blocking between Greenland and western Europe correspond to a warmer, more saline subpolar ocean. The correspondence between blocked westerly winds and warm ocean holds in recent decadal episodes (especially, 1996-2010). It also describes much longer-timescale Atlantic multidecadal ocean variability (AMV), including the extreme, pre-greenhouse-gas, northern warming of the 1930s-1960s. The space-time structure of the wind forcing associated with a blocked regime leads to weaker ocean gyres and weaker heat-exchange, both of which contribute to the warm phase of AMV.

The climate of the global oceans undergoes natural variability with many time-scales, as well as greenhouse-induced change. We discuss the relationship between periods of warm subpolar ocean and patterns of blocking in the atmospheric circulation above in the North Atlantic sector. Blocking occurs when the high-latitude jet stream develops large, nearly stationary meanders, essentially breaking Rossby waves with precursors upwind, over North America. These trap an air mass equatorward of an anticyclonic pressure ridge. We show here that clusters of frequent blocking over the subpolar North Atlantic coincide with warm and saline ocean in the 1960s, late 1970s and early 2000s (*1*). Further back in time, a new reconstruction of surface atmospheric pressure field for the entire 20th Century (*2,3*) encompasses the most dramatic climate event of the Century: the pre-greenhouse-gas northern warming that began in the 1920s and lasted until the 1960s. Sea-surface temperatures (SST) of the North Atlantic also show this wide spread warming while the South Atlantic Ocean is cooler than normal. This longer time-scale variability is known as Atlantic Multidecadal Variability (AMV, or Atlantic Meridional Oscillation, AMO)(*4,5*). AMV has been linked to many multi-decadal climate processes: Atlantic hurricanes, NE Brazil and Sahel rainfall, North American and European summer climate (*5-7*). We show below that warm ocean and frequent atmospheric blocking coincide, over multidecadal AMV timescales. More than a local response to the atmosphere, invasions of warm ocean water northward from the subtropics, extending well below the surface, are involved (*1,8).*

Atmospheric blocking involves shifts in Atlantic storm tracks lasting several days. Blocking over Greenland is associated with the negative phase of the North Atlantic

Oscillation (NAO) and a southward shift of the storm track (*9*) (Fig. S1). The blocking also occurs further east over western Europe with an anticyclone over the northern subpolar gyre (Fig. S2). Such blocking is accompanied with cold winter temperatures in western Europe, for example winters 2005/06 (*10)*, and 1963 and 2009/2010 (*11*). The climatological maximum in winter blocking days is located over western Europe with a secondary maximum over Greenland connected by a ridge of increased blocking (Fig. S3), if blocking is defined by absolute geopotential height index (*12*; which is an extension of *13; 14)*. Thus the east-west location of Atlantic blocking anticyclones varies, but in 61 of 110 cases investigated in (*9*), European blocks immediately precede Greenland blocks.

Changes in the storm track impact the ocean circulation through surface wind-stress and wind-stress curl. Wind-stress curl causes downward (in the subtropics) or upward (subpolar) pumping of surface waters, driving the circulation gyres. The particularly strong episode of subpolar warming and salinization in the early 2000s was associated with weakening of wind-stress curl, hence weakened gyre circulation, and decreased heat loss over the subpolar Atlantic (*1*). And indeed, the long decline of subpolar gyre surface currents from 1994 to 2000 revealed by satellite altimetry (*15*) corresponds with a weakening wind-curl field.

Indices of wind-related climate variability are based on Empirical Orthogonal Function (EOF; (*14*)) analysis of the winter (December-March) wind-stress curl, using the recently produced 20th century reanalysis (and the 60-year NCEP/NCAR Reanalysis for comparison). Both datasets give essentially the same spatial EOF patterns and amplitudes shown in Fig. 1a. EOF1 has an extremum west of Ireland, centered on the

boundary between the subpolar and subtropical ocean gyres, and its time series (principal component, PC, in Fig. 1b) correlates highly with the NAO-index. EOF2 (Fig. 1a) has extrema co-located with the ocean gyres and its time series, PC2, is shown Fig. 1b. EOF2 represents weakening and strengthening the climatological-mean pattern and hence the strength of the gyre circulation. PC time series from NCEP/NCAR reanalysis data for the latter half of the century follow closely the 20th century reanalysis results.

For the recent decades, 1960-2005, the PC2 time series of the wind stress curl was found to be the key index associated with the saline and warm periods in the northern North Atlantic Ocean because it controls the expansion/contraction and strength of both subpolar and subtropical gyres (*1*). With a longer atmospheric reanalysis we can now address climate regimes associated with the SST variability such as the AMV focusing on the wind stress curl PC2 of the EOF analysis. To highlight the North Atlantic climate regimes we computed sea level pressure (SLP), blocking, and turbulent heat-flux anomalies based on composited differences between negative and positive events in wind stress curl PC2 (>1 standard deviation) (*14*). All analysis results displayed are based on the 20th century reanalysis data.

The number of wintertime blocking days (from December to March) was determined from the ensemble-mean daily 500hPa height data. The mean annual blocking days over a decade (Fig. 2a) use the definition (*12*) based on north-south dynamic height gradient at 500hPa over the latitude range 34N-74N at each longitudinal grid point in the Atlantic sector, and requiring persistence of 5 or more days (*14*). The

20th century reanalysis tends to overestimate blocking days in the latter half of the century compared with the NCEP/NCAR in the overlapping period (Fig. S4). However the temporal and spatial fluctuations are similar, such as wide-spread blocking activity in the 1960s and 2000s, weak blocking in the 1980s and 1990s, and two centers of activity in the 1950s. NCEP/NCAR Reanalysis singles out the late 1960s as the most unusual period with persistent blocking at every longitude between western Europe and Greenland (Fig. S5). Despite the differences between the reanalyses, some decades display more blocking activity than others (Fig. 2a). The warmest periods occur in the North Atlantic Ocean when increased blocking occurs over the Western Europe and has an extension towards Greenland, i.e., 1920-1970, and after 2000. This association is evident in the time series of blocked days in the subpolar Atlantic (Fig. 2b) and AMO-index of subpolar ocean surface temperature (as in (*7, 14*)), with and without the trend removed. The difference between full and detrended AMO-index shows the importance of the global warming signal in the recent years (*7*).

Wind-stress curl, EOF mode 2, has the same spatial pattern as the mean ocean gyres; we call EOF2/PC2 the 'gyre mode'. It is distinct from the NAO, which more resembles EOF1. Wind-stress curl relates to the vorticity of the winds, hence to the Laplacian of SLP which emphasizes smaller-scale features than SLP-based analysis (*16-18)*: an SLP-composite corresponding to negative minus positive curl PC2 events results in a pattern (Fig. 3a) resembling the Eastern Atlantic pattern in SLP-EOF analysis (*12, 19*), and also the Atlantic-Ridge pattern found with cluster analysis (*16, 17*). This SLP pattern has been identified as a blocking signature (*12*). This pattern was also recovered as an SLP difference-field of warm years 1939-1968 minus cold years of 1900-1929 (*20*).

With different binning of the warm (1950-1964) and cold (1970-1984) years the SLP pattern resembles more the negative NAO pressure anomaly (*21*). The multidecadal depth-dependent AMV temperature mode found in the zonal average is also linked to the Eastern Atlantic SLP pattern (*8*). There is no spatial similarity between the NAO pattern and the wind curl EOF2, and the PC2 is not strongly correlated with the NAO index, but the PC2 time series shows remarkably close relationship with the subpolar SLP anomaly (Fig. 3b) and, less significantly, with the subtropical Azores SLP center. The relationship between the low frequency Azores SLP and ocean gyre variability has been found from analysis of the sea level variability along the European coast (*22*).

To establish the linkage between the wind stress curl variability and blocking we form composited difference fields using the wind-stress curl PCs. The composite of anomalous blocking activity based on PC1 (Fig. S6, as negative minus positive PC1 events) corresponds to Greenland blocking known to be associated with the negative NAO phase (*18*). On the other hand, the PC2 composites (again as negative minus positive PC2 events, Fig. 4a) show simultaneously increased activity of the western European blocking and a weaker Greenland blocking, flanked by decreased blocking over Scandinavia and Southern Europe. This specific blocking anomaly reaching from Greenland to western Europe represents fluctuations of the climatological-mean blocking pattern (Fig. S3) with contributions from positive and negative NAO index, where the NAO-positive contributions occur over the eastern side of the North Atlantic and western Europe. Extending the classic NAO description of North Atlantic atmospheric

variability, by allowing east-west displacement of centers of action in this way, is suggested in earlier work (*9*, *17*).

The active blocking band from Greenland to the western Europe was also seen in decadal variability of the extended early-midcentury warm period (Fig. 2). Using the same years as in (*20*) to define warm period (1939-1968) and cold period (1900-1929), the resulting difference in blocking days (Fig. 4b) has an anomaly of increased blocking from Greenland to Europe very similar to that corresponding to the curl PC2 (Fig. 4a). The areas of significance (95% or higher, 58 degrees of freedom) are stippled. Using the AMO index (with no detrending) to form a composite (positive minus negative) of the blocking events (Fig. S7) gives the same band of increased blocking as the wind stress curl PC2 although with somewhat less significance.

In addition to the association of warm, saline ocean with weakening of the wind-stress curl and subpolar and subtropical gyre circulation, air-sea heat flux influences SST. The composite difference of turbulent (sensible and latent) heat flux corresponding to (negative minus positive) curl PC2 (Fig. 4c) shows the heat flux anomaly associated with the climate regimes which have weak circulation gyres and high blocking activity. This heat flux anomaly favors heating in large part of the North Atlantic including the Equatorial region with weak cooling in a narrow band in the mid-latitudes. This heating anomaly pattern differs from that corresponding to the NAO index, where the subpolar heating/cooling is centered over the Labrador Sea (instead of the central subpolar gyre)

and the cooling/heating over the Gulf Stream region is of the same order of magnitude as in the Labrador Sea.

Fig. 4 shows that a similar blocking activity can be recovered whether using the gyre index (wind stress curl PC2) or multidecadal SST variability as the compositing index. This is an implication that the particular blocking anomaly is fundamental part of the forcing of the gyre variability at low frequencies. Moreover it is associated with surface heat exchange which supports heat content variability, in turn amplifying the effects of expanding and contracting ocean gyres.

In summary, variability of atmospheric blocking over years to several decades shows correlation with the ocean surface temperature and with significant changes in Atlantic Ocean circulation, mediated by wind-stress curl and air-sea heat exchange. The wind-stress curl variability of most importance for the subpolar gyre represents weakening/strengthening of the climatological-mean curl pattern (*1*). This same mode of variability is associated with a major shift in the upper ocean currents after year 2000 and warming and salinization of the subpolar gyre (*1*, *23*). Wind-stress curl variability represents changes in the Atlantic storm track, storm frequency and intensity, and particularly persistent events, i.e. blocking, where storm tracks are shifted, have a large impact on the curl. For example with negative NAO-index, a block over southern Greenland forces the existence of single upper level mid-latitude jet crossing the Atlantic (*18*). However, the index of our wind stress curl pattern, the gyre mode, is not correlating strongly with NAO, nor projects purely on Greenland blocking but contains a large

component of blocking centered on western Europe. Increased activity of both Greenland and western Europe blocking centers has occurred when the North Atlantic has been in a warm state. The gyre mode also supports atmosphere-ocean heat exchange, which sustains a warm state of the North Atlantic, from the subpolar region through most of the subtropics to the Equator. This suggests that blocking activity is more fundamental than the NAO-index in describing climatic changes in the Atlantic Ocean.

The blocking events (lasting 5 days or more) provide an example of high-frequency atmospheric variability projecting on lower frequency variability of the wind-stress curl. Winters with frequent blocking appear to persist for decades, and are evidence of a highly disturbed hemispheric jet stream system. We speculate that the westerly wind-stress directed along the Gulf Stream/North Atlantic Current system is less intense and less coherent in such conditions. Our analysis cannot separate cause and effect between high blocking activity and warm ocean surface but the existing theory of the mid-latitude atmosphere-ocean interaction supports increased persistence of atmospheric anomalies that created oceanic anomalies in the first place (*24*). Warm-ocean/cold-land anomaly-pattern has been linked to a dynamical environment favorable for blocking *(25-26)*. Blocking has also been shown to be sensitive to a warmer subpolar Atlantic in a reconstruction of the cold European winter of 2005-6 *(10)*. The possibility of coupled interaction of atmosphere with Atlantic Multi-decadal Variability seems likely, given the long-period variability of blocking reported here, and in the even longer paleo-climate time series (*27*). AMV has been attributed to changes in the Atlantic Meridional Overturning Circulation (AMOC) in some numerical model experiments (*28*,

29). Also, based on hydrographic data, AMV exhibits vertical structure, which could signal AMOC variability (*8*). Clearly, feedbacks between the hemispheric jet-stream waveguide, tropical and extra-tropical ocean temperatures and the AMOC itself are possible and even likely.

References:

1. S. Häkkinen, P.B. Rhines and D.L. Worthen, Warm and saline events embedded in the meridional circulation of the northern North Atlantic. J. Geophys. Res., **116,** C03006, doi:10.1029/2010JC006275 (2011).

2. G. P. Compo, J.S. Whitaker, and P.D. Sardeshmukh, Feasibility of a 100 year reanalysis using only surface pressure data. Bull. Amer. Met. Soc., **87**, 175-190, (2006).

3. G. P. Compo, *et al.*, The Twentieth Century Reanalysis Project. Q. J. R. Meteorol. Soc., **137**, 1-28 (2011).

4. D. B. Enfield, A.M. Mestaz-Nunez, and P.J. Trimble, The Atlantic multi-decadal oscillation and its relation to rainfall and river flows in the Continental US. Geophys. Res. Lett., **28**, 2077-2080 (2001).

5. K. E. Trenberth, and D.J. Shea, Atlantic hurricanes and natural variability in 2005. Geophys. Res. Lett., **33**, L12704, doi:10.10129/2006GL026894 (2006).

6. J. R. Knight, C. K. Folland, and A. A. Scaife, Climate impacts of the Atlantic Multi-decadal Oscillation. Geophys. Res. Lett., **33**, L17706, doi:10.1029/2006GL026242 (2006).

7. M. Ting, Y. Kushnir, R. Seager, and C. Li, Forced and Internal Twentieth-Century SST Trends in the North Atlantic, J. Clim., **22**, 1469-1481 (2009).

8. I. V. Polyakov, V.A. Alexeev, U.S. Bhatt, E.I. Polyakova and X. Zhang, North Atlantic warming: patterns of long-term trend and multidecadal variability. Clim. Dyn., **34**, 439-457 (2010).

9. T. Woollings, B. J. Hoskins, M. Blackburn and P. Berrisford, A new Rossby-wave breaking interpretation of the North Atlantic Oscillation. J. Atmos. Sci. **65**, 609-626

(2008).

10. M. Croci-Maspoli and H.C. Davies, Key dynamical features of the 2005/06 European winter. Mon. Wea. Rev., **137**, 664-678 (2009).

11. J. Cattiaux *et al*., Winter 2010 in Europe: A cold extreme in a warming climate. Geophys. Res. Lett., **37**, L20704, doi:10.1029/2010GL044613 (2010).

12. S. C. Scherrer, M. Croci-Maspoli, C. Schwierz and C. Appenzeller, Two-dimensional indices of atmospheric blocking and their statistical relationship with winter climate patterns in the Euro-Atlantic region. Int. J. Climatol., **26**, 233-249 (2006).

13. S. Tibaldi, and F. Molteni, On the operational predictability of blocking. Tellus, **42A**, 343-365 (1990).

14. Supporting material on data sets and methods on *Science* Online.

15. S. Häkkinen, and P.B. Rhines, Decline of subpolar North Atlantic gyre circulation during the 1990s. Science, **304**, 555-559 (2004).

16. C. Cassou, L. Terray, J.W. Hurrell and C. Deser, North Atlantic winter climate regimes: spatial symmetry, stationarity with time and oceanic forcing. J. Clim., **17**, 1055-1068 (2004).

17. J. W. Hurrell, and C. Deser, North Atlantic climate variability: The role of the North Atlantic Oscillation. J. Mar. Syst., **79**, 231-244 (2010).

18. T. Woollings, A. Hannach, B. Hoskins, and A. Turner, A regime view of the North Atlantic Oscillation and its response to anthropogenic forcing. J. Clim., **23**, 1291-1307 (2010).

19. M. Croci-Maspoli, C. Schwierz, and H.C. Davies, Atmospheric blocking: space-time links to NAO and PNA. Clim. Dyn., **29**, 713-725 (2007).

20. C. Deser and M.L. Blackmon, Surface climate variations over the North Atlantic Ocean during winter: 1900-1989. J. Clim., **6**, 1743-1753 (1993).

21. Y. Kushnir, Interdecadal variations in North Atlantic sea surface temperature and associated atmospheric conditions. J. Clim., **7**, 141-157 (1994).

22. L. Miller, and B.C. Douglas, Gyre-scale atmospheric pressure variations and their relation to 19th and 20th century sea level rise. Geophys. Res. Lett., **34**, L16602, doi: 10.1029/2007GL030862 (2007).

23. S. Häkkinen, and. P.B. Rhines, Shifting surface currents of the northern North Atlantic Ocean. J. Geophys. Res., **114**, doi:10.1029/2008JC004883 (2009).

24. J. J. Barsugli, and D.S. Battisti, The basic effects of atmosphere-ocean thermal coupling on midlatitude variability. J. Atm. Sci., **55**, 477-493 (1998).

25. A. Shabbar, J. Huang and K. Higuchi, The relationship between the wintertime North Atlantic Oscillation and blocking episodes in the North Atlantic. Int. J. Climatol., **21**, 355-369 (2001).

26. D. Barriopedro, R. Garcia-Herrera, A.R. Lupo and E. Hernandez, A climatology of Northern Hemisphere Blocking. J. Clim, **19**, 1042-1063 (2006).

27. E. Rimbu, and G. Lohmann, Winter and summer blocking variability in the North Atlantic region – evidence from long-term observational and proxy data from southwestern Greenland. Clim. Past Disc. **5**, 2411-2437 (2009).

28. T.L. Delworth, and M.E. Mann, Observed and simulated multidecadal variability in the Northern Hemisphere, Clim. Dyn., **16**, 661-676 (2000).

29. J. R. Knight, C. K. Folland, and A. A. Scaife, Climate impacts of the Atlantic Multidecadal Oscillation. Geophys. Res. Lett., **33**, L17706, doi:10.1029/2006GL026242

(2006).

30. R.W. Preisendorfer, 1988: Principal Component Analysis in Meteorology and Oceanography. Developments in Atmospheric Science, 17. Elsevier Amsterdam.

Supporting Online Material

www.sciencemag.org

Materials and Methods

Figs. S1-S7

Reference (30) [Note: The numbers refer to any additional references cited only within the SOM]

Acknowledgements

SH and DLW were funded by NASA Headquarters Physical Oceanography Program and OSTM Science Team. PBR is supported by NASA through the OSTST Science Team. We thank our reviewers for constructive criticism.

Figure Captions

Figure 1. The winter (December-March) wind stress curl variability from the 20th century atmospheric reanalysis based on EOF analysis.

(a) spatial pattern of wind stress curl EOF1 and EOF2. EOF1 (top) represents 22.3% of the wind stress curl variability, and has its centers of action displaced north-south relative to the subpolar ocean gyre. EOF2 (bottom panel) with 15.6% of the variance has centers of action coinciding with the subpolar and northern subtropical ocean gyres.

(b) Principal components of wind stress curl EOFs from the 20th century reanalysis. PC1 (red), PC2 (blue), and from NCEP/NCAR Reanalysis PC1(dashed black), and PC2 (dashed purple). The standard deviation of the PC2 from the 20th century reanalysis is 8.9 10^{-8} Nm^{-3} (includes interannual variability). Time series are smoothed by 10 binomial filters.

Figure 2. (a) Mean winter (DJFM) blocking days by decade from the 20th century reanalysis. (b) DJFM Blocking days in the region 10°E-70°W, 45°N-75°N from the 20th century reanalysis (black curve) and from NCEP/NCAR Reanalysis (blue curve). The two blocking time series have a correlation of 0.85 over the overlapping time period 1949-2008. The AMO-index (dashed pink curve) is an area-averaged SST from 0°N-60°N, 10°E-80°W. The AMO index with global surface temperature evolution removed (as in (*7*)) shown as a solid red curve. The SST curves are smoothed by 3 binomial filters.

Figure 3. Relationship between the gyre index and SLP. Analysis period is 1901-2008. (a) Composite difference of SLP based on negative minus positive wind stress curl PC2 events stronger than one standard deviation shows the SLP anomaly associated with a

weakened subpolar gyre. Color denotes SLP anomaly in hPa. Stippling denotes significance of difference at 95% level.

(b) Subpolar SLP (blue) (average over 20W-50W, 50N-65N) and curl PC2 (red) from the 20th century reanalysis smoothed by 10 binomial filters.

Figure 4. Anomaly patterns of blocking activity. Analysis period is 1901-2008.

(a) Composite difference of blocking days based on negative minus positive curl PC2 events stronger than one standard deviation shows the increased blocking occurring from Greenland to western Europe when the subpolar gyre is weak. Stippling denotes significance of difference at 95% level.

(b) Warm (1939-1968) minus cold years (1900-1929) (as defined in (*20*)) difference in blocking days. Stippling denotes significance of difference at 95% level assuming 58 degrees of freedom.

(c) Anomaly of the surface heat exchange associated with the gyre index. Composite difference of turbulent heat flux (positive upward; color denotes flux magnitude in units of Wm^{-2}) based on negative minus positive curl PC2 events stronger than one standard deviation shows the wide spread heat input to the ocean when the gyre circulation is also weak. Stippling denotes significance of difference at 95% level.

Figures:

(a)

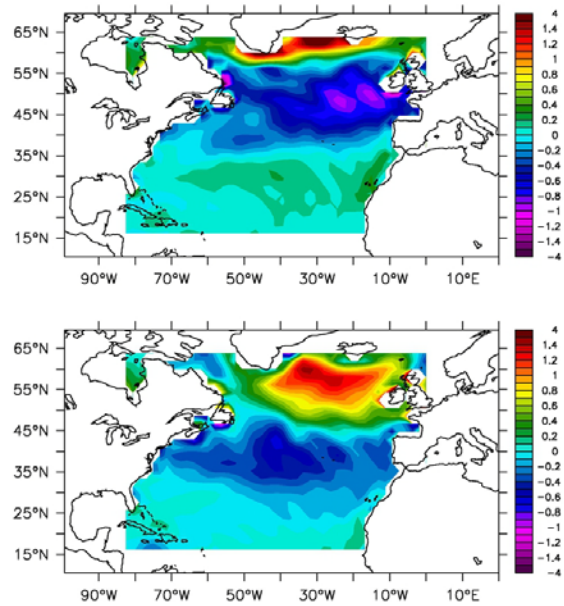

(b)

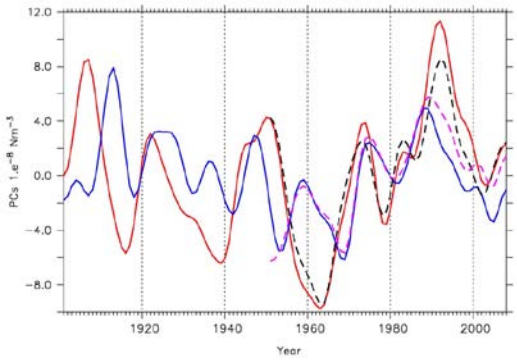

Figure 1. The winter (December-March) wind stress curl variability from the 20th century atmospheric reanalysis based on EOF analysis.
(a) spatial pattern of wind stress curl EOF1 and EOF2. EOF1 (top) represents 22.3% of the wind stress curl variability, and has its centers of action displaced north-south relative to the subpolar ocean gyre. EOF2 (bottom panel) with 15.6% of the variance has centers of action coinciding with the subpolar and northern subtropical ocean gyres.
(b) Principal components of wind stress curl EOFs from the 20th century reanalysis. PC1 (red), PC2 (blue), and from NCEP/NCAR Reanalysis PC1(dashed black), and PC2 (dashed purple). The standard deviation of the PC2 from the 20th century reanalysis is 8.9 10^{-8} Nm^{-3} (includes interannual variability). Time series are smoothed by 10 binomial filters.

(a)

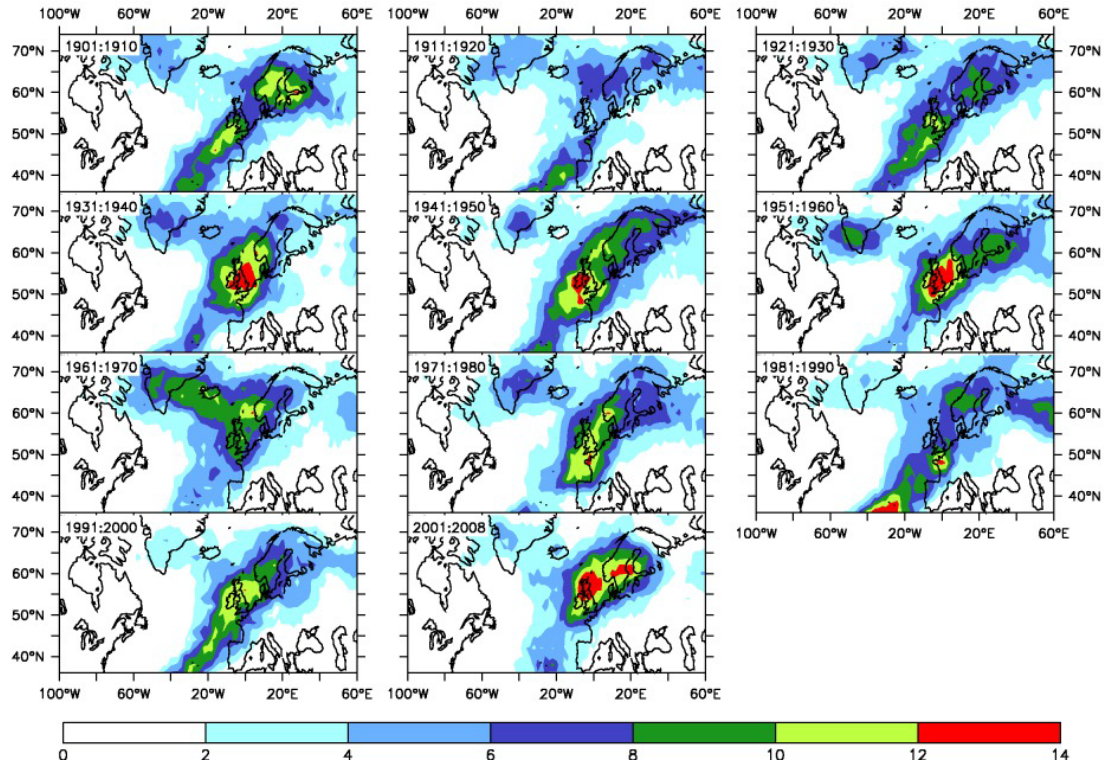

(b)

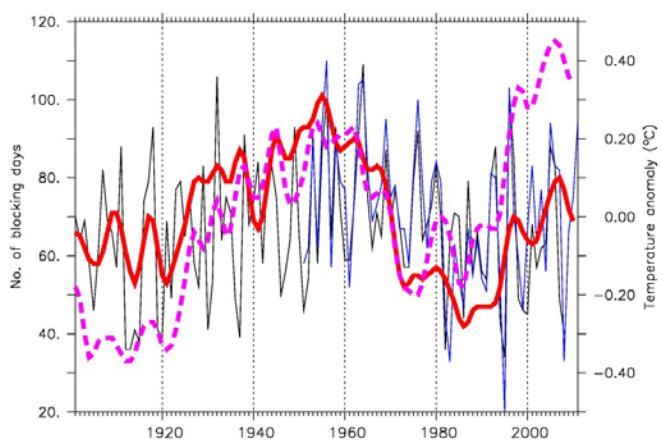

Figure 2. (a) Mean winter (DJFM) blocking days by decade from the 20th century reanalysis. (b) DJFM Blocking days in the region 10°E-70°W, 45°N-75°N from the 20th century reanalysis (black curve) and from NCEP/NCAR Reanalysis (blue curve). The two blocking time series have a correlation of 0.85 over the overlapping time period 1949-2008. The AMO-index (dashed pink curve) is an area-averaged SST from 0°N-60°N, 10°E-80°W. The AMO index with global surface temperature evolution removed (as in (*7*)) shown as a solid red curve. The SST curves are smoothed by 3 binomial filters.

(a)

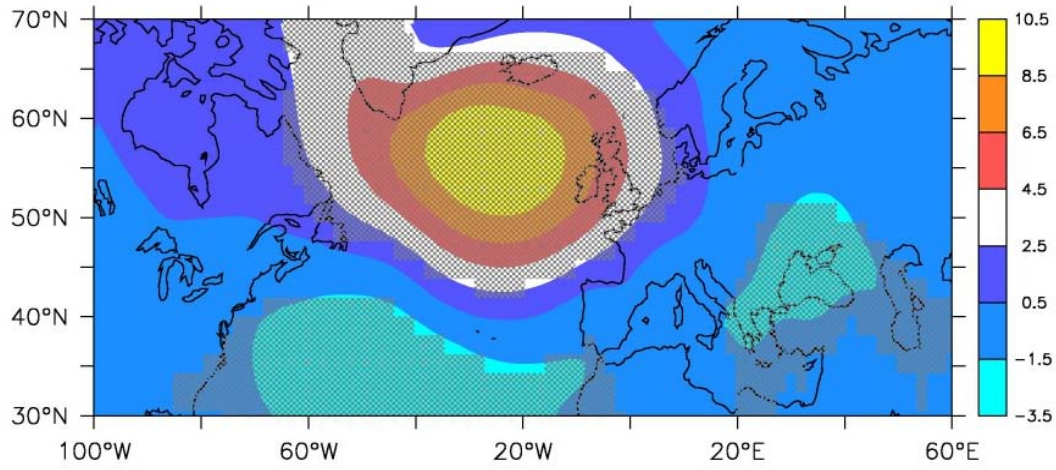

(b)

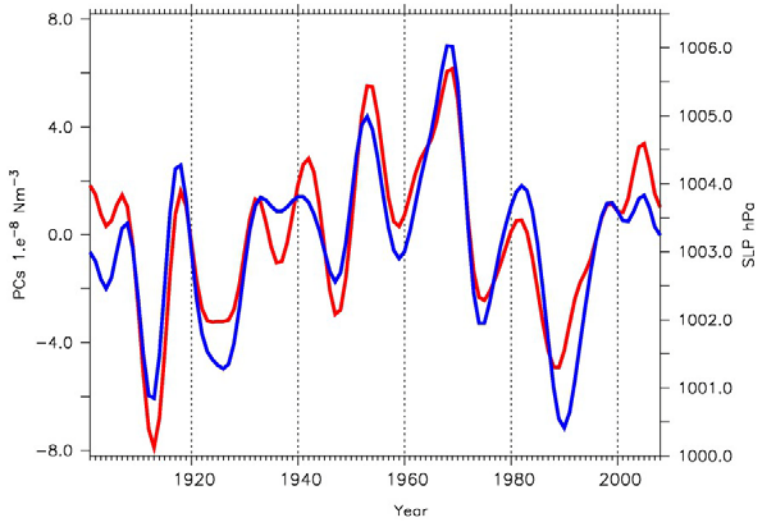

Figure 3. Relationship between the gyre index and SLP. Analysis period is 1901-2008. (a) Composite difference of SLP based on negative minus positive wind stress curl PC2 events stronger than one standard deviation shows the SLP anomaly associated with a weakened subpolar gyre. Color denotes SLP anomaly in hPa. Stippling denotes significance of difference at 95% level.
(b) Subpolar SLP (blue) (average over 20W-50W, 50N-65N) and curl PC2 (red) from the 20th century reanalysis smoothed by 10 binomial filters.

(a)-(b)

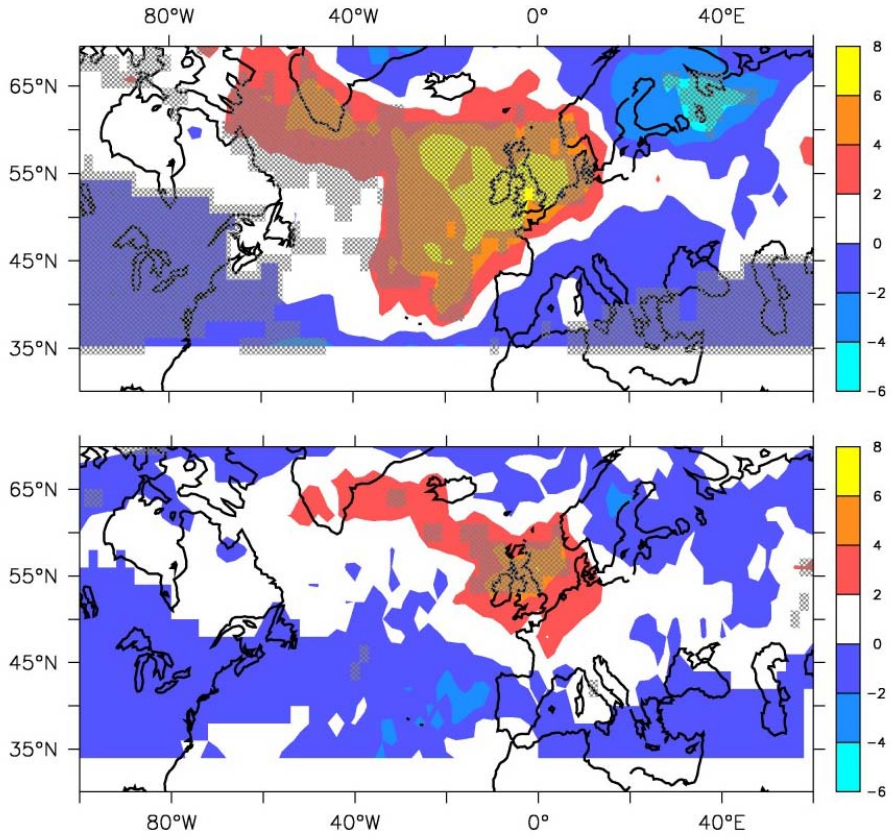

(c)

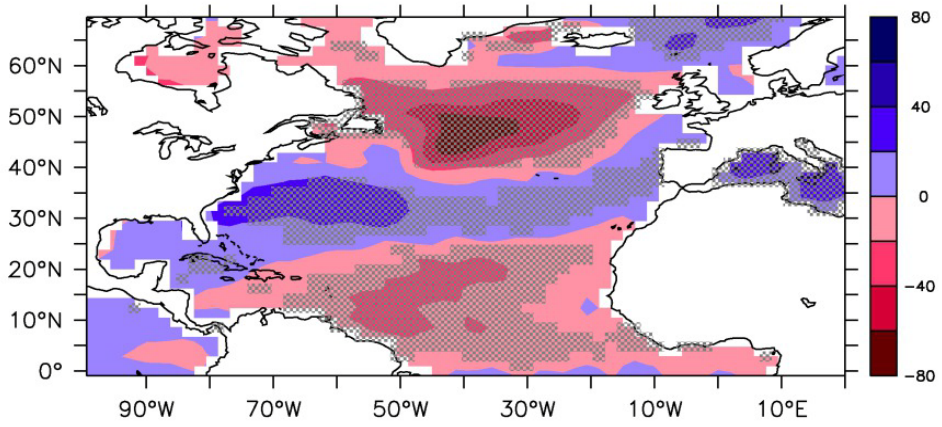

Figure 4. Anomaly patterns of blocking activity. Analysis period is 1901-2008.

(a) Composite difference of blocking days based on negative minus positive curl PC2 events stronger than one standard deviation shows the increased blocking occurring from Greenland to western Europe when the subpolar gyre is weak. Analysis period is 1901-2008. Stippling denotes significance of difference at 95% level.
(b) Warm (1939-1968) minus cold years (1900-1929) (as defined in (*20*)) difference in blocking days. Stippling denotes significance of difference at 95% level assuming 58 degrees of freedom.
(c) Anomaly of the surface heat exchange associated with the gyre index. Composite difference of turbulent heat flux (positive upward; color denotes flux magnitude in units of Wm^{-2}) based on negative minus positive curl PC2 events stronger than one standard deviation, showing wide-spread heat input to the ocean when the gyre circulation is weak. Stippling denotes 95% significance-level.

Supporting Online Material for

Atmospheric Blocking and Atlantic Multi-decadal Ocean Variability

Sirpa Häkkinen, Peter B. Rhines and Denise L. Worthen.

correspondence to: sirpa.hakkinen@nasa.gov

This PDF file includes:

Materials and Methods
SOM Text
Figs. S1 to S7

Materials and Methods

Data sets utilized:

The 20th Century Reanalysis (*2,3*)which is an ensemble mean of 56 realizations of an experimental version of NCEP global forecast model assimilating only surface pressure reports and using observed monthly sea-surface temperature and sea-ice distributions as boundary conditions. It is available at:
http://www.esrl.noaa.gov/psd/data/gridded/data.20thC_ReanV2.html
We also used NCEP/NCAR Reanalysis which is available at:
http://www.esrl.noaa.gov/psd/data/gridded/data.ncep.reanalysis.html
Hadley SST (HadISST = Hadley sea ice and sea surface temperature) used to compute AMO Index as an area weighted average over (0-60N, 10E-70W). Hadley surface temperatures (HadCRUT3) averaged over (60S to 60N) were used to compute the forced temperature ('global warming') signal contributing to the AMO variability as suggested in (*7*) : First AMO is regressed onto the global average surface temperature; then the Atlantic multidecadal variability arises as a residual after the global warming contribution is subtracted off. Both data sets are available from: http://www.hadobs.org/ .

Methods:

Empirical Orthogonal Function (EOF) analysis (*28*). EOFs analysis separates the space-time data fields into a set of spatial functions and their time series (or principal components, PCs). Time series of various modes are not correlated at lag 0 by the definition.

Computation of the blocking days:

Here we follow (*12*) to compute two geopotential height gradients at 500hPa for each latitude and longitude grid point in the Atlantic sector:

$GHGN = (Z(\lambda,\phi_N) - Z(\lambda,\phi_0)) / (\phi_N - \phi_0) < -10$ (m/ degrees of latitude) ,

$GHGS = (Z(\lambda,\phi_0) - Z(\lambda,\phi_S)) / (\phi_0 - \phi_S) > 0$,

Z is the 500hPa height, λ is longitude, ϕ_0, ϕ_N and ϕ_S are the center, northern and southern latitudes respectively, and $|\phi_0 - \phi_{N/S}| = 16$ degrees (the 20th century analysis has 2 degree resolution). With this choice we can compute blocking days for latitude range 34ºN to 74ºN. We require that these gradient conditions are fulfilled at least for 5 days in a grid point to qualify as a blocked grid point.

Composite analysis of SLP, blocking days and heat flux. We chose to create composited differences instead of correlations because compositing includes nonlinearities present in the data sets. The events (winters here) chosen to the composite are based on an index time series such as the wind stress curl PC2 where we search PC2 values, which exceed one standard deviation of both negative and positive sign. We then group e.g. the SLP fields corresponding to the negative and positive PC2 extremes. We form a composite by subtracting the fields associated with the positive extremes of PC2 from the fields associated with the negative extremes of PC2 (we chose the negative – positive PC2 because it reflects the weak

gyres and increased blocking). The significance of the difference field is tested using t-distribution with (n1+n2-2) degrees of freedom where n1 and n2 are number of fields corresponding to the negative and positive PC2 extremes with sample means of $\underline{x1}$ and $\underline{x2}$. The population variance is estimated based on

$s^2 = [\Sigma (x1 - \underline{x1})^2 + \Sigma (x2 - \underline{x2})^2] / (n1+n2-2)$, finally

the t-test statistic to be computed is

$[(\underline{x2} - \underline{x1}) - 0] / [s \sqrt{(1/n1 + 1/n2)}]$

We chose to use 95% significance to shade the composited difference fields.

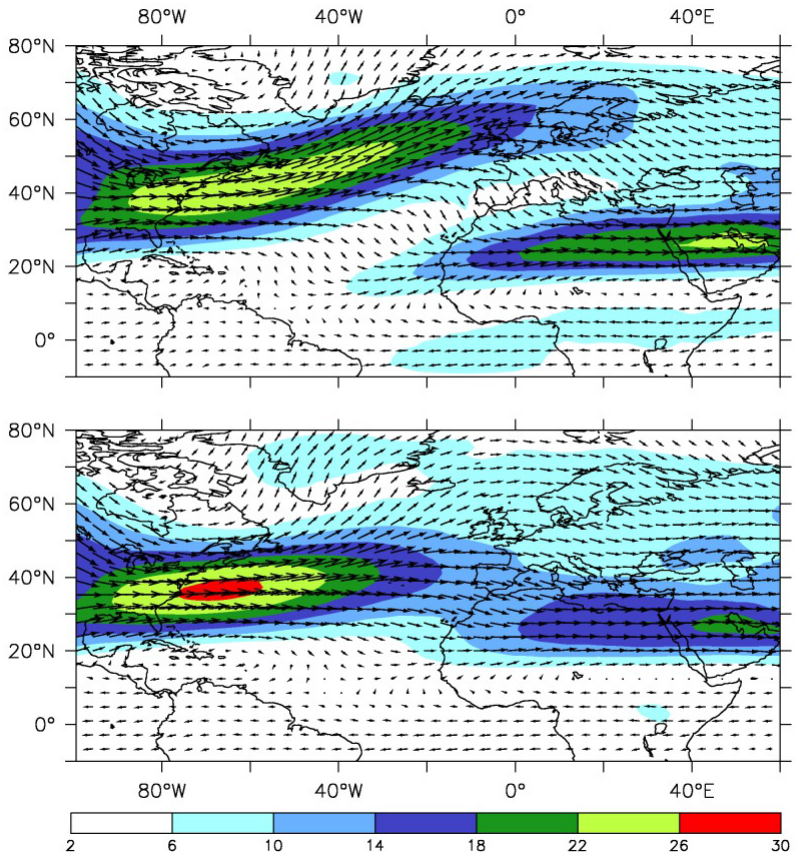

Fig. S1. The 500hPa wind (magnitude given in color; units in m/s) composites corresponding to positive (top) and negative (bottom) wind stress curl PC1 (a proxy to positive and negative NAO). The upper figure shows the unblocked regime dominated by the subpolar jet, i.e. storm track. The lower figure shows the blocked regime with a continuous jet crossing at subtropical latitudes and with a non-existent subpolar jet. Analysis period is 1901-2008.

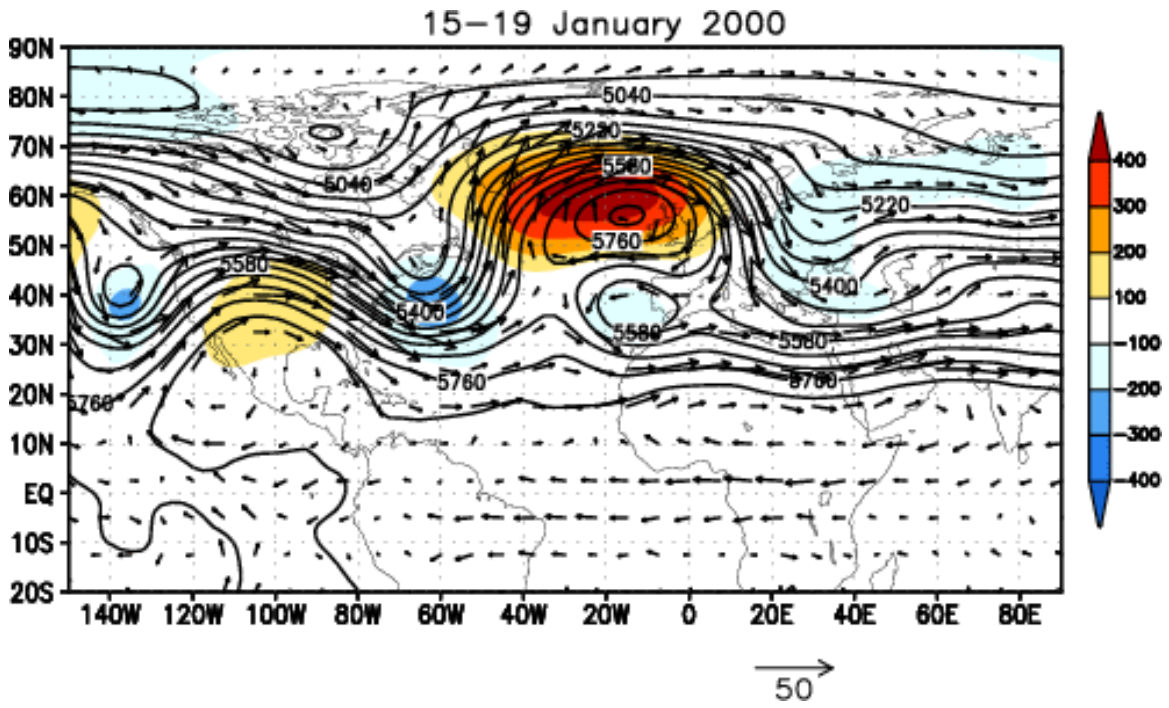

Fig. S2. Example of western European blocking from NCEP analysis. 500hPa geopotential height (contours; m), and its anomalies (color; m) show the anticyclone over the northern Atlantic and the reversals of the geopotential height gradient between the longitudes 40W and 0. The atmospheric flow is diverted around it with an intense flow from north bringing cold air to Europe. From http://www.cpc.ncep.noaa.gov/products/precip/CWlink/blocking/background/atlantic_case.shtml

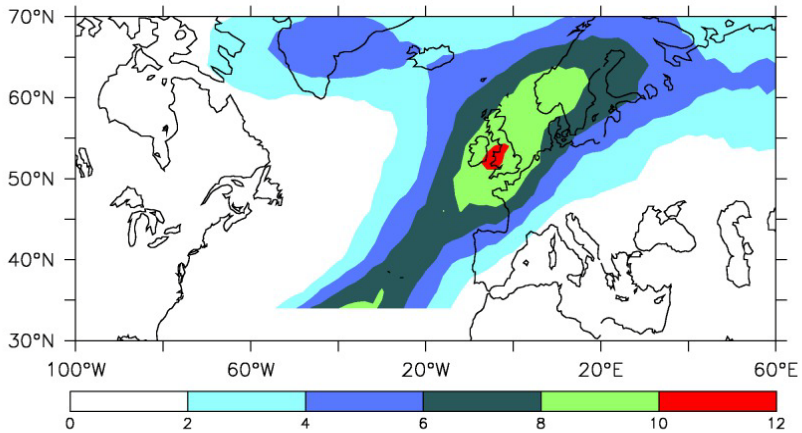

Fig. S3. Climatological number of blocking days in December-March season from the 20th century reanalysis for analysis period of 1901-2008.

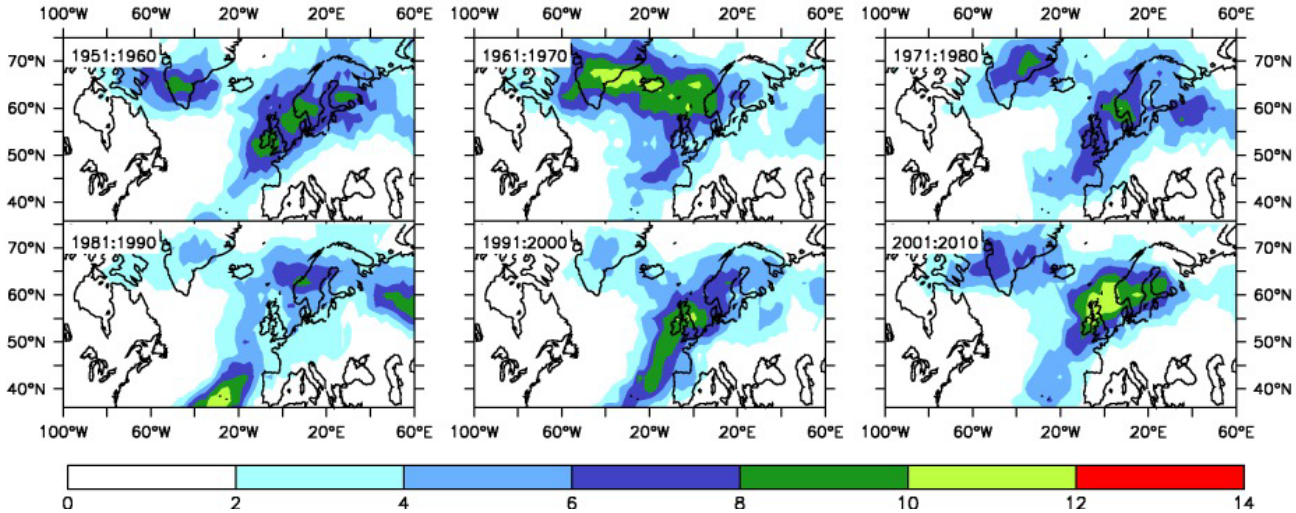

Fig. S4. Mean winter (DJFM) blocking days per decade from the NCEP/NCAR reanalysis.

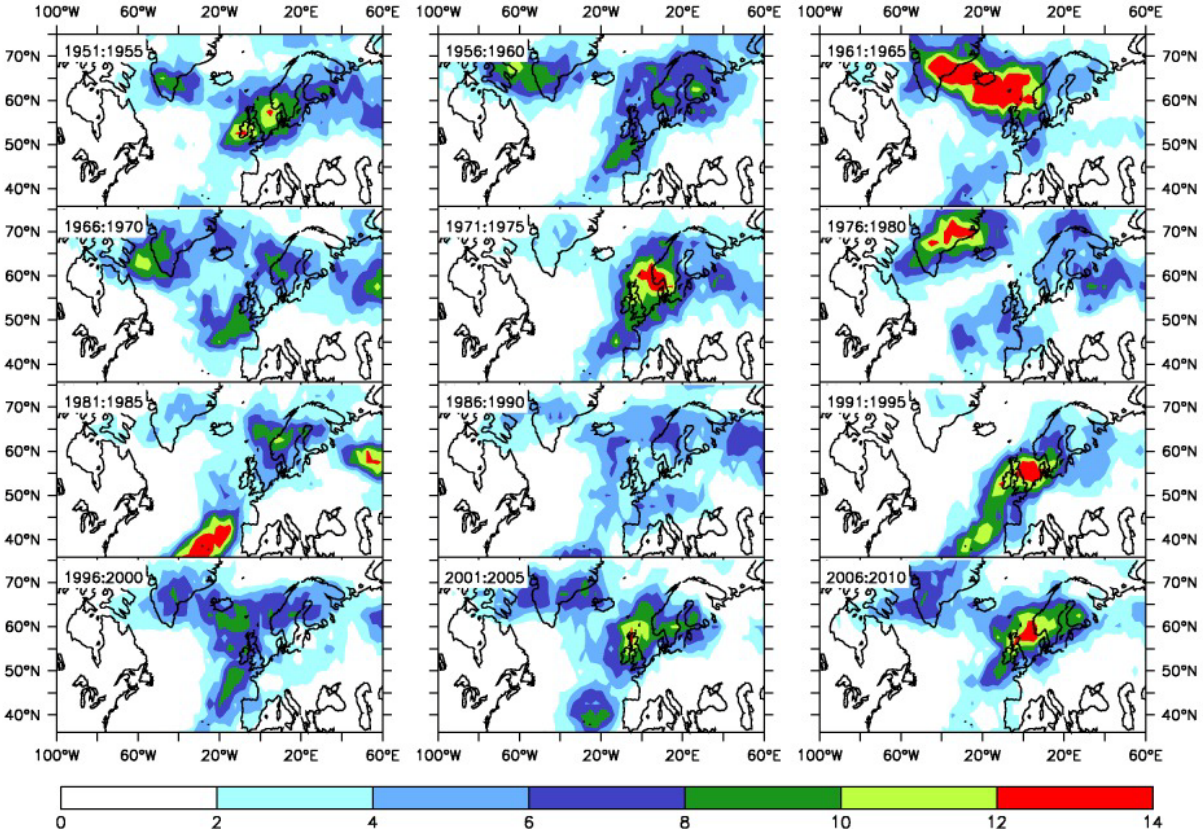

Fig. S5. Mean winter (DJFM) blocking days per pentad from the NCEP/NCAR reanalysis.

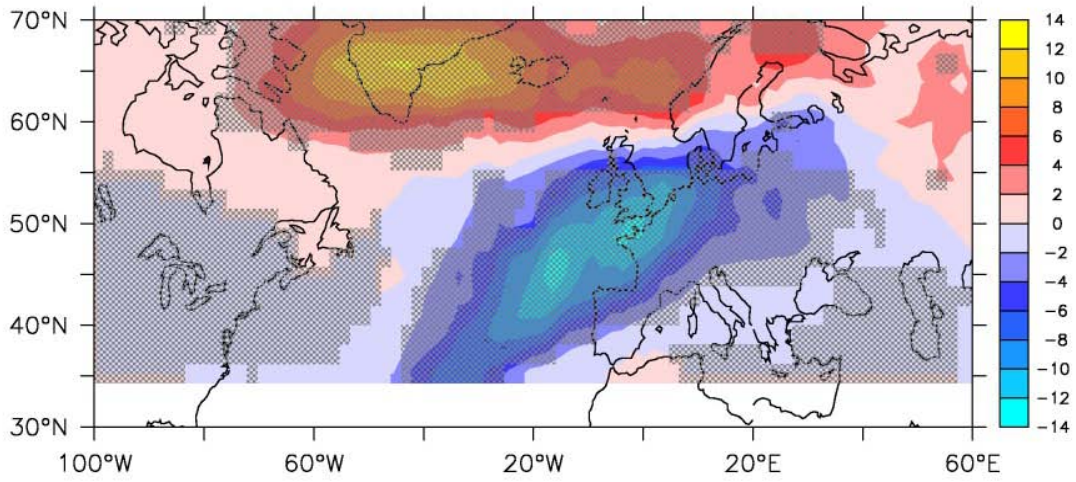

Fig. S6. Composite of anomalous winter blocking days based on negative minus positive wind stress curl PC1 (proxy for negative NAO minus positive NAO) events stronger than one standard deviation. Pattern shows the increased blocking over the Greenland associated with negative NAO and weaker blocking over the western Europe. Analysis period is 1901-2008. Stippling denotes significance of difference at 95% level.

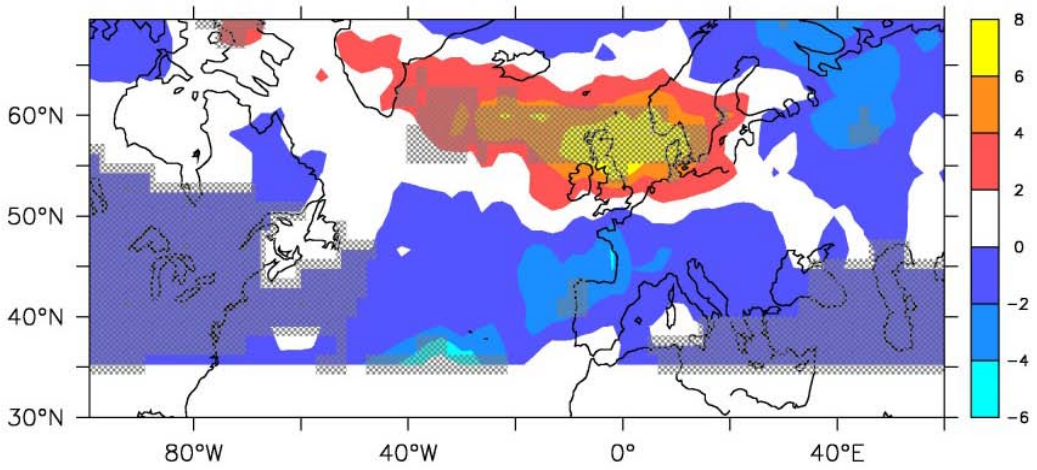

Fig. S7. Composite of anomalous blocking days based on positive minus negative AMO-index events (includes the global warming signal, the dashed curve in Fig. 2b) stronger than one standard deviation. Analysis period is 1901-2008. Stippling denotes significance of difference at 95% level.